Predicting Catastrophic Phase Inversion on the Basis of Droplet Coalescence Kinetics

G. E. J. Vaessen, M. Visschers, and H. N. Stein*

Laboratory of Colloid Chemistry and Thermodynamics, Faculty of Chemical Technology, Eindhoven University of Technology, P.O. Box 513, 5600 MB Eindhoven, The Netherlands

Received May 15, 1995. In Final Form: October 10, 1995[⊗]

A predictive model for catastrophic phase inversion, based on the kinetics of droplet breakup and coalescence, is presented here. Two inversion mechanisms can be distinguished, depending on the direction of the phase inversion process. With the surfactant predominantly present in the dispersed phase, the coalescence rate is high and "easy" phase inversion takes place at relatively low volume fractions. Going in the other direction, surfactant is predominantly present in the continuous phase. The coalescence rate is dramatically lowered because of the Gibbs−Marangoni effect, and "difficult" inversion will not take place up to relatively high volume fractions. Experiments were carried out in a stirred vessel, where phase inversion was detected by a jump in emulsion conductivity. Easy inversion points were found on the order of 20−50% volume fraction of the dispersed phase. Difficult inversion was not detected up to 97% dispersed phase. The easy inversion point increases with dispersed phase addition rate and is independent of the stirrer speed below a stirrer speed of 1500 rpm. A simple model based on the breakup and coalescence rate of emulsion droplets in the easy inversion regime allows us to calculate the stationary droplet size as a function of the volume fraction of the dispersed phase, as well as the evolution of the droplet size in time under addition of dispersed phase. The stationary droplet size diverges above a critical volume fraction of 26.4%, indicating phase inversion. This model can qualitatively describe hysteresis and the phase inversion point dependence on stirrer speed and dispersed phase addition rate, as found in our experiments.

Introduction

The term *catastrophic phase inversion* was introduced by Salager[1] to indicate phase inversion in emulsions induced by increasing the volume fraction of dispersed phase, as opposed to *transitional inversion*, induced by changing the surfactant distribution over the phases. This term was chosen after Dickinson[2] had pointed out that emulsion phase inversion, induced by increasing the volume fraction of the dispersed phase, shows the characteristics of a catastrophe (in the mathematical sense), in particular hysteresis. It was further suggested that catastrophe theory, a mathematical framework to describe catastrophic processes, would be applicable to phase inversion. However, Vaessen and Stein[3] recently pointed out that catastrophic phase inversion in emulsions does not satisfy basic prepositions of catastrophe theory and suggest that this type of inversion should be modeled on the basis of coalescence kinetics.

Phase inversion processes similar to catastrophic inversion in emulsions have been found in liquid−liquid dispersions (i.e., in the absence of an emulsifying agent).[4] Arashmid and Jeffreys[5] formulated a predictive model for phase inversion. They assumed that inversion would take place when every collision of drops would result in coalescence. Employing an estimate of the collision frequency from Misek,[6] an empirical estimate of the net coalescence frequency in liquid−liquid dispersions from Howarth,[7] and an estimate of the Sauter mean diameter of the drops from Thornton and Bouyotiotes,[8] they developed an equation with just one adjustable parameter describing the inversion point as a function of stirrer speed. Their prediction agreed quite well with experimental data, although it has been argued that incorrect expressions were used to derive their predictive equation.[9]

We will not go into a discussion about the choice of estimates in the model of Arashmid and Jeffreys, but we will try to apply their idea to phase inversion in emulsions. It is arguable to apply concepts developed in the field of liquid−liquid dispersions to emulsions, since their behavior is very different: emulsions, while formally unstable, may display metastable behavior over considerable time. This is caused by the fact that the surfactant layer around the droplets delays the drainage process of the film between two collided droplets considerably, resulting in a very low coalescence efficiency. In liquid−liquid dispersions, on the other hand, this retarding mechanism is absent, coalescence efficiency is high, and these dispersions usually separate within a short time after agitation has stopped.

It has, however, been pointed out by Traykov and Ivanov[10] that emulsion droplets will under certain conditions coalesce very rapidly, with an efficiency in the range of that of nonstabilized drops. We will show in this paper that these particular conditions rule for a certain type of catastrophic phase inversion and present a tentative predictive model for phase inversion, based on the kinetics of coalescence processes.

Two Inversion Mechanisms

In transitional inversion, the curvature of the oil−water interface changes more or less gradually from positive to

[⊗] Abstract published in *Advance ACS Abstracts,* January 1, 1996.

(1) Salager, J. L. In *Encyclopedia of Emulsion Science*; Becher, P., Ed.; Marcel Dekker: New York, 1988; Vol. 3, p 79.
(2) Dickinson, E. *J. Colloid Interface Sci.* **1981**, *84*, 284.
(3) Vaessen, G. E. J.: Stein, H. N. *J. Colloid Interface Sci.*, in press.
(4) McClarey, M. J.; Mansoori, G. A. *AIChE Symp. Ser.* **1987**, *74*, 134.
(5) Arashmid, M.; Jeffreys, G. V. *AIChE J.* **1980**, *26*, 51.
(6) Misek, T. *Collect. Czech. Chem. Commun.* **1964**, *29*, 2086.
(7) Howarth, W. J. *AIChE J.* **1967**, *13*, 1007.
(8) Thornton, J. D.; Bouyotiotes, B. A. *Inst. Chem. Eng. Symp. Ser.* **1967**, *26*, 43.
(9) Guilinger, T. R.; Grislingas, A. K.; Erga, O. *Ind. Eng. Chem. Res.* **1988**, *27*, 978.
(10) Traykov, T. T.; Ivanov, I. B. *Int. J. Multiphase Flow* **1977**, *3*, 471.
(11) Shinoda, K.; Kunieda, H. In *Encyclopedia of Emulsion Technology*; Becher, P., Ed.; Marcel Dekker: New York, 1983; Vol. 1, Chapter 5.

0743-7463/96/2412-0875$12.00/0

negative or vice versa. The system will pass through a state of zero average curvature, a bicontinuous state.[11] In catastrophic inversion, such a bicontinuous intermediate state does not exist. The essential step in the phase inversion process is the rapid coalescence of droplets throughout the whole system, to form the new continuous phase. The coalescence process itself can roughly be divided into three stages: (1) collision of two droplets, (2) drainage of the film between the droplets, and (3) rupture of the film. In most cases, the drainage of the film (stage 2) is the rate-determining step. Already more than a century ago, Reynolds[12] presented an equation for the thinning rate of a film between two rigid, parallel disks:

$$V_0 = \frac{2h^3\Delta P}{3\mu_c a^2} \tag{1}$$

where ΔP represents the driving force of the thinning process per unit area. This pressure may be caused by an external force or by capillary suction from the plateau border. At later stages of drainage, this pressure may be opposed by repulsive interaction forces of electrostatic or steric nature, usually represented by means of a disjoining pressure Π.

Reynolds's equation was applied with success to describe thinning rates in emulsion films, where the rigid disk assumption seemed to hold quite well. In foam films, and in liquid−liquid films in absence of surfactant, however, much greater thinning rates have been found experimentally. This effect was attributed to the mobility of the boundaries enclosing the film. Ivanov and Traykov[13] presented a hydrodynamic theory by solving the Navier−Stokes equation, taking into account the flow both in the film and in the droplets. For steady flow in a symmetrical film they find

$$\frac{V}{V_0} = 1 + \frac{1}{\epsilon^e} \tag{2}$$

with V_0 the Reynolds drainage velocity, as given by eq 1, and

$$\epsilon^e = \frac{2}{3B}\left(\frac{\rho h^4 \Delta P}{a^2}\right)^{1/3}\frac{\mu_d^{1/3}}{\mu_c} \tag{3}$$

In a following paper,[10] a similar analysis was presented for emulsion films, taking into account the Gibbs−Marangoni effect:

$$\frac{V}{V_0} = 1 + \frac{1}{\epsilon^e + e^f} \tag{4}$$

with

$$\epsilon^f = -\frac{(\partial\sigma_0/\partial c_{0,c})\,\Gamma_0}{3\mu_c D_c\left[1 + \frac{2D_s(\partial\Gamma_0/\partial c_{0,c})}{D_c h}\right]} \tag{5}$$

and ϵ^e and V_0 as given by eqs 3 and 1, respectively.

As can be seen from eq 5, ϵ^f is nonzero only if there is surfactant present in the continuous phase (i.e., in the film). Typical values are $\epsilon^e \ll 1$ and $\epsilon^f \gg 1$ for surfactant soluble in the phase forming the film, i.e., the continuous phase. In this case, $V \approx V_0$, i.e., the Reynolds equation predicts the drainage rate quite accurately. With the surfactant present in the droplet phase, $\epsilon^e \ll 1$ and $\epsilon^f = 0$, resulting in $V \gg V_0$, the same result as for pure liquid−liquid dispersions.

This analysis confirms Bancroft's rule: droplets made up of the phase containing surfactant are much less stable than droplets surrounded by this phase. Therefore, the most stable morphology is the one in which the surfactant is present in the continuous phase. These two coalescence regimes are linked to two different regimes for catastrophic phase inversion. Salager defined the terms *normal* and *abnormal* emulsions:[1] in a normal emulsion, the surfactant is present in the continuous phase; the morphology of this emulsion is its preferred morphology, determined by Bancroft's rule. An abnormal emulsion has a nonpreferred morphology, with the surfactant present in the dispersed phase. Inversion from an abnormal to a normal emulsion will involve "rapid" film drainage, with $V \gg V_0$. Inversion from a normal to an abnormal emulsion will involve "slow" film drainage, with $V \approx V_0$.

Vaessen and Stein[14] presented two mechanisms for catastrophic phase inversion. "Easy" inversion takes place in abnormal emulsions. The driving process is rapid coalescence (eq 4) with $\epsilon^e \ll 1$ and $\epsilon^f = 0$) and is opposed by breakup of the emulsion droplets. Before phase inversion, there is a dynamic balance between coalescence and breakup: droplets that grow too large break up easily, and droplets that become too small coalesce. Since breakup is a unary process, proportional to the number of droplets per unit volume, and coalescence is a binary process, proportional to the number of droplets per unit volume *squared*, the coalescence rate increases faster than the breakup rate with increasing volume fraction of the dispersed phase. At a certain point, the dynamic balance between coalescence and breakup will collapse, and phase inversion will occur.

The other mechanism, "difficult" inversion, may take place in normal emulsions. The driving force is now "slow" coalescence (eq 4) with $\epsilon^e \ll 1$ and $\epsilon^f \gg 1$). Because the coalescence efficiency is so much lower in this case, the balance between breakup and coalescence will hold until much higher volume fractions of the dispersed phase. The efficiency may be so low that the films remain intact even beyond the point of closest packing of spherical droplets. A liquid−liquid foam will be formed, where film drainage is not only slowed down by transport of continuous phase *through* the film but also *away from* the film. Because of the even lower drainage rate, inversion may not take place until extremely high volume fractions are reached. Ofter such high volume fractions cannot be reached in practice, since it becomes very difficult to mix additional dispersed phase with the emulsion or to extract the remaining continuous phase from it. The two different inversion mechanisms described above may be the reason for the occurrence of hysteresis in catastrophic phase inversion.

Theory and Calculations

Vaessen and Stein[14] presented a simple model to estimate the volume fraction of the dispersed phase at which easy phase inversion would take place. This model was based on the evolution of the stationary (average) droplet size of an emulsion with increasing volume fraction of the dispersed phase. The stationary droplet size was estimated by finding the droplet size for which coalescence and breakup are balanced, i.e., they do not change the number mean droplet size.

(12) Reynolds, O. *Philos. Trans. R. Soc. London* **1886**, *A177*, 157.
(13) Ivanov, I. B.; Traykov, T. T. *Int. J. Multiphase Flow* **1976**, *2*, 397

(14) Vaessen, G. E. J.; Stein, H. N. *Proceedings of the First World Congress on Emulsion*; Congres Mondial de l'Emulsion: Paris, 1993; Vol. 1, paper no. 1-30-102.

Some basic assumptions underlie the model by Vaessen and Stein:[14] the degree of agitation, expressed by either the shear rate in the viscous regime or the turbulent energy dissipation in the inertial regime is assumed to be independent of the position in the emulsifying equipment. Furthermore, the equipment is considered to be completely wetted by the continuous phase. In cases of incomplete wetting, the phase inversion point may become dependent on the material of the emulsifying equipment.[15] The most essential assumption in the model is that the coalescence efficiency is taken equal to one, i.e., that every collision results in coalescence. Although within the view of the rapid coalescence regime involved in easy inversion this assumption is not unreasonable, it may seem completely in contradiction with the inversion criterion employed by Arashmid and Jeffreys,[5] namely, that inversion would take place when every collision results in coalescence. At first sight, breakup is not accounted for in the model by Arashmid and Jeffreys. However, the expression for coalescence frequency by Howarth[7] they employed is based on the rate of change of the number of droplets in a dispersion and, therefore, on the net effect of coalescence and breakup. The point where the net coalescence rate equals the collision rate of drops is equal to the point where breakup is overruled by coalescence and the stationary droplet size diverges. Thus, the inversion criteria applied by Arashmid and Jeffreys[5] and Vaessen and Stein[14] are equivalent.

Vaessen and Stein[14] used expressions for the coalescence and breakup rate in the viscous regime, corresponding to their experiments with a high-viscosity resin as the continuous phase. In this paper, we present experiments in a low-viscosity system, with droplet sizes typically larger than the Kolmogorov length scale. Hence, appropriate expressions for the inertial regime should be employed. The coalescence rate is taken from Saffman and Turner:[16]

$$R_c(d) = 6.87\epsilon^{1/3}d^{7/3}n(d)^2 \tag{6}$$

and the breakup rate from Delichatsios and Probstein:[17]

$$R_b(d) = 1.37\sqrt{\frac{2}{\pi}}\epsilon^{1/3}d^{-2/3}\exp\left(\frac{\sigma}{1.88\epsilon^{2/3}d^{5/3}}\right)n(d) \tag{7}$$

$n(d)$ represents the number of droplets of diameter d, and the energy dissipation rate ϵ is given by[18]

$$\epsilon = C_1 D_{imp}{}^2 N_{imp}{}^3 \tag{8}$$

where C_1 is a constant of order unity.

Coalescence and breakup rates were calculated from eqs 6 and 7 as a function of the droplet size. An estimate for the stationary droplet size was then determined by bisection, finding the droplet size at which coalescence and breakup do not change the number mean diameter. The stationary droplet size was calculated as a function of the volume fraction of the dispersed phase, for three values of the stirrer speed: 1000, 2000, and 3000 rpm. Other values employed are $D_{imp} = 0.0432$ m, $C_1 = 1$, $\sigma = 10^{-2}$ N/m, and $\rho = 998$ kg/m^3. The results are presented in Figure 1. At a volume fraction of 0.264, the stationary droplet size diverges, and phase inversion or phase separation occurs. The phase inversion point appears to be independent of the stirrer speed in the range employed here.

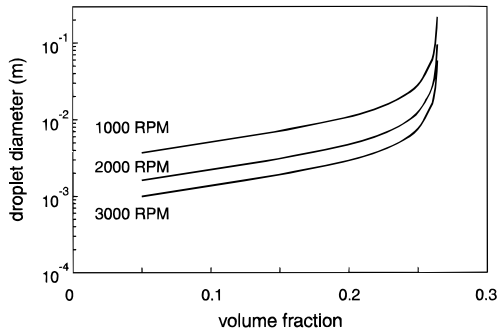

Figure 1. Calculations of the stationary droplet size in the easy inversion regime.

When applying the above method to "difficult" inversion, involving slow coalescence, a coalescence efficiency <1 has to be accounted for. Chesters[19] proposed the derivation of the coalescence efficiency from the ratio between the interaction time of approaching droplets and the drainage time of the film between them:

$$P = e^{-t_d/t_i} \tag{9}$$

The interaction time t_i may be estimated from the time for two particles to pass each other in turbulent flow:

$$t_i \sim d^{2/3}\epsilon^{-1/3} \tag{10}$$

In reality, the interaction time will show a stronger dependence on the droplet size due to the fact that droplets may bounce instead of pass each other. This effect is neglected here.

The drainage time can be found solving the Reynolds's drainage equation (1), which now appears in the form

$$V = -\frac{dh}{dt} = \frac{32\pi\sigma^2h^3}{3\mu_c d^2F} \tag{11}$$

where the driving force is represented by F, mainly due to the (turbulent) flow pressing the two droplets together. Since this force determines the degree of flattening of the droplets, the radius of the flattened area, a, could be eliminated from eq 1 by applying $F \sim \pi a^2 4\sigma/d$. The solution of eq 11 is

$$t_d = \frac{3\mu_c d^2F}{64\pi\sigma^2}\left(\frac{1}{h_c{}^2} - \frac{1}{h_0{}^2}\right) \tag{12}$$

where h_0 is the film thickness at $t = 0$ and h_c is the critical thickness of the film at which rupture occurs. The beginning of the drainage process, $t = 0$, is assumed to be the moment that the drainage velocity from eq 11 equals the approach velocity of two droplets in turbulent flow:

$$v \sim (\epsilon d)^{1/3} \tag{13}$$

As the film thins, the London–Van der Waals attractive forces will increase. When these interaction forces balance the hydrodynamic pressure in the film (for flattened droplets equal to the Laplace pressure), the film will rupture and coalescence will take place. The critical film thickness is given by[19]

(15) Davies, J. T.; Rideal, E. K. *Interfacial Phenomena,* 2nd ed.; Academic Press: New York, 1963; pp 378–383.
(16) Saffman, P. G.; Turner, J. S. *J. Fluid Mech.* **1956**, *1*, 16.
(17) Delichatsios, M. A.; Probstein, R. F. *Ind. Eng. Chem. Fundam.* **1976**, *15*, 134.
(18) Narsimhan, G.; Gupta, J. P.; Ramkrishna, D. *Chem. Eng. Sci.* **1979**, *34*, 257.
(19) Chesters, A. K. *Chem. Eng. Res. Des.* **1991**, *69*, 259.

$$h_c \sim \left(\frac{Ad}{16\pi\sigma}\right)^{1/3} \tag{14}$$

The external force F, in the inertial regime, can be estimated by

$$F \sim \rho v^2 d^2 \sim \rho \epsilon^{2/3} d^{8/3} \tag{15}$$

Equation 15 represents the external hydrodynamic interaction force only. In the later stages of film thinning, other interaction forces (electrostatic, steric, and Van der Waals) may also enter the force balance between the droplets. These interaction forces are usually represented in the form of a disjoining pressure Π:

$$\Pi = \Pi_{\text{electrostatic}} + \Pi_{\text{steric}} + \Pi_{\text{Van der Waals}} \tag{16}$$

The Van der Waals contribution to the disjoining pressure has already implicitly entered this analysis by means of eq 14. We can neglect the steric contribution, since the molecular weight of the surfactant we used is only 485 (vide infra, Experimental Section). The electrostatic contribution to the disjoining pressure, for a symmetrical plane geometry, is given by[20]

$$\Pi_{\text{electrostatic}} = 2n_0 kT\left(\cosh\frac{ze\psi_m}{kT} - 1\right) \tag{17}$$

with ψ_m the electrical potential midway between the two charged plates. An accurate equation for ψ_m was given by Gregory:[21]

$$\sinh\frac{ze\psi_m}{kT} = \frac{ze\psi_0}{kT}\,\text{cosech}(\kappa h/2) \tag{18}$$

where ψ_0 is the surface potential and κ the Debye−Hückel parameter given by

$$\kappa = \left(\frac{2z^2e^2n_0}{\epsilon_0\epsilon_r kT}\right)^{1/2} \tag{19}$$

for a symmetrical electrolyte.

Following eq 18, the electrostatic pressure increases very rapidly with decreasing film thicknesses. The hydrodynamic pressure, on the other hand, will never exceed the Laplace pressure $4\sigma/d$. If the electrostatic pressure is negligible with respect to the hydrodynamic pressure at the critical film thickness, h_c, it will be negligible throughout the whole drainage process. In our experiments, we have used nonionic surfactants and a relatively high salt concentration. Therefore, it is expected that the surface potential is relatively small. We will use a value of $|\psi_0| = 25$ mV. Other values employed are $\sigma = 10^{-2}$ N/m, $A = 10^{-20}$ J, $\rho = 10^3$ kg/m^3, $\epsilon = 10$ m^2/s^3 (corresponding to 1050 rpm), $n_0 = 4 \times 10^{25}$ m^{-3} (corresponding to 5 g/L KCl, vide infra, Experimental Section), $\epsilon_r = 80$, $T = 298$ K, and $z = 1$. With these values, using eqs 14−19, it can be calculated that for $d > 1.2 \times 10^{-5}$ m the maximum electrostatic pressure, at critical thickness, is smaller than the Laplace pressure. Since the electrostatic pressure decreases dramatically with increasing film thickness, it is a reasonable approximation to neglect the electrostatic pressure for $d > 1.2 \times 10^{-5}$ m.

There is one more assumption to be verified in this analysis: the Reynolds's drainage equation (eq 11) is only valid for flat films. Approaching droplets will form a flat film when the pressure building up between the droplets becomes equal to the Laplace pressure. Chesters[19] derives an expression for h_{flat}, the film thickness at which the onset of flattening takes place:

$$h_{\text{flat}} \sim \frac{F}{2\pi\sigma} \tag{20}$$

Since the drainage velocity is proportional to h^3 (eq 11), the last stages of the drainage process are rate-limiting. The use of the Reynolds drainage equation is therefore justified if the film will have flattened before rupture takes place, i.e., if $h_{\text{flat}} > h_c$. From eqs 14 and 20, with $\sigma = 10^{-2}$ N/m, $A = 10^{-20}$ J, $\rho = 10^3$ kg/m^3, and $\epsilon = 10$ m^2/s^3, it can be calculated that this is the case for $d > 1.3 \times 10^{-5}$ m.

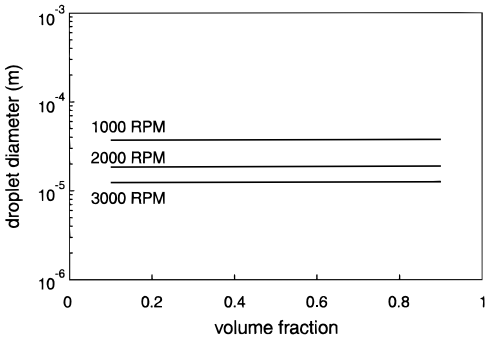

Figure 2. Calculations of the stationary droplet size in the difficult inversion regime.

Using eqs 9−15, the coalescence rate calculated from (6) can be corrected for the coalescence efficiency. Following the same approach as for easy inversion, the stationary droplet size as a function of the volume fraction of the dispersed phase was calculated. The results are presented in Figure 2. Comparing figures 1 and 2, droplet sizes are an order of magnitude smaller in the case of difficult inversion, and divergence of the droplet size (i.e., phase inversion) is not predicted. The calculations show hysteresis in catastrophic phase inversion as a result of the different inversion mechanisms involved. It should, however, be noted that eqs 6 and 7, used in our calculations, are valid only in the low volume fraction regime, and no accurate conclusions can be drawn for the behavior of emulsions at higher volume fractions. The accuracy of the calculated droplet sizes is also limited by the fact that, at a stirrer speed of 3000 rpm, these are on the order of 1.2×10^{-5} m, the critical limit for assuming flat film drainage and neglecting the electrostatic interaction pressure.

For easy inversion, the model described above allows us to predict more than the stationary droplet size alone. It can also be used to follow the evolution of the average droplet size in time. At $t = 0$ we start with a monodisperse distribution of droplets of a certain diameter d_0. Over a small time step Δt, we assume the number concentration of drops to be constant. Equations 6 and 7 then give the decrease of the number of drops of size d_0 and the number of drops formed by coalescence (size $2^{1/3}d_0$) or by breakup (size $2^{-1/3}d_0$). From this distribution, a number mean diameter d_1 is calculated, after which the distribution is again assumed monodisperse, now with diameter d_1. This process is repeated many times until convergence or divergence of the number mean diameter. Below the inversion point, the number mean diameter converges to exactly the same value as found by bisection, provided the time step Δt is sufficiently small, allowing us to determine the time needed for convergence. Above the inversion point, we can get an indication of the time needed for the stationary droplet size to diverge by setting an

(20) Verwey, E. J. W.; Overbeek, J. Th. G. *Theory of the Stability of Lyophobic Colloids*; Elsevier: Amsterdam, 1948.
(21) Gregory, J. *J. Chem. Soc., Faraday Trans. 2* **1973**, *69*, 1723.

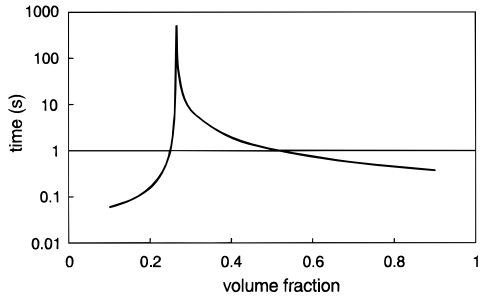

Figure 3. Calculations of the time needed for the droplet size to converge (below the phase inversion point) or to diverge (above the phase inversion point).

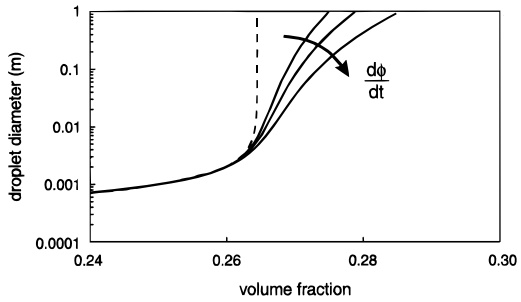

Figure 4. Calculations of the evolution of the droplet size with increasing volume fraction. Solid lines: droplet size evolution at dispersed phase addition rates of 0.0002, 0.0004, and 0.0008 s^{-1}, increasing in the direction of the arrow. Broken line: stationary droplet size.

arbitrary criterion for divergence of the droplet diameter, d_{div}. Calculations have been performed for easy inversion with a stirrer speed of 1500 rpm, using $d_0 = 10^{-4}$ m, $\Delta t = 10^{-4}$ s, and $d_{div} = 1$ m. Results are presented in Figure 3.

Approaching the inversion point, the time needed to reach the stationary droplet size diverges dramatically. Also, slightly above the inversion point, the droplet size diverges very slowly, causing a delay in phase inversion. Further beyond the inversion point, the delay time decreases rapidly. Delayed phase inversion has been observed experimentally by Gilchrist et al.[22]

Many phase inversion experiments involve adding dispersed phase to an emulsion under stirring. Knowing the droplet size evolution with time at the inversion point, we can model the effect of the addition rate of dispersed phase. Again, we consider small time steps Δt, in which we calculate the change in number mean droplet diameter from d_t to $d_{t+\Delta t}$. Starting with a low volume fraction at $t = 0$, it is incremented every time step by $\Delta\phi = (d\phi/dt)\Delta t$. We can now follow the droplet size as a function of the volume fraction. Results are shown in Figure 4, for addition rates $d\phi/dt = 0.0002$, 0.0004, and 0.0008 s^{-1} and further settings identical to those in the delay time calculations. Also shown in Figure 4 is the stationary droplet size (for 1500 rpm).

From Figure 4 it can be seen that until close to the inversion point the stationary droplet size is reached very quickly, independent of the addition rate. As soon as the stationary droplet size diverges, the actual droplet size starts increasing, but not as rapidly. There is a clear overshoot of the stationary inversion point, which becomes larger with increasing addition rate. Hence, the dynamic inversion point will shift to higher volume fractions at higher addition rates.

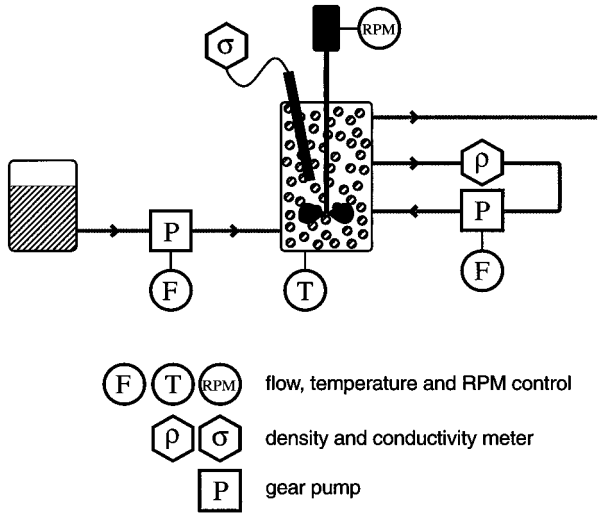

Figure 5. Layout of the experimental setup.

Experimental Section

Phase inversion experiments were carried out in a stirred vessel, in which the morphology of the emulsion was measured by means of conductivity. The experimental setup is shown in Figure 5. At the beginning of the experiment, the continuous phase with a certain concentration of surfactant is present in the vessel. Dispersed phase, containing exactly the same concentration of surfactant, is pumped into a vessel by means of a gear pump Verder Micro V004, at a constant flow rate. Excess emulsion flows out of the vessel; therefore, the volume fraction increases in time according to the continuous stirred tank reactor (CSTR) equation:

$$\phi(t) = 1 - e^{-t/\tau} \tag{21}$$

where τ is the residence time in the vessel.

The stirrer motor, IKA RE 162, is equipped with rpm control, to ensure a constant stirrer speed. This is especially important close to the inversion point, where the viscosity of the emulsion may increase dramatically.[23] The volume fraction of water in the emulsion is measured by use of a Paar density meter DMA 55 with an external flow cell DMA 401 (4 digit accuracy). To measure the density, the emulsion is continuously pumped through a bypass by another gear pump. The flow rate of the bypass pump and the volume of the bypass tubing are such that the residence time in the bypass is about 3 orders of magnitude smaller than the residence time in the vessel.

A more detailed picture of the vessel is shown in Figure 6, and the dimensions are given in Table 1. The vessel is partly double-walled and was thermostated at 20 °C in all experiments. The stirrer is a four-blade stainless steel propeller. The rectangular blades are tilted such that the propeller pumps downwards. To avoid rotation of the liquid in the vessel, four stainless steel baffles are present. Conductivity is measured in the vessel by a four-electrode cell, Philips PW 9571.

The surfactant, used in our experiments, is nonylphenol hexaethoxylate, Synperonic NP6 ex ICI (average molecular weight 485). The aqueous phase (further indicated as the water phase) is double-distilled water, to which 5 g/L KCl p.a. ex Merck was added to obtain a better contrast in conductivity. The organic phase (further indicated as the oil phase) was *n*-hexane ex Caldic. Inversion experiments were carried out in both directions (water added to oil and oil added to water).

To both phases was added 1 g/L surfactant. The advantage of this method, consistent with the experimental work of other researchers in this field,[24,25] is that the overall surfactant concentration is constant throughout the inversion experiment. A disadvantage is that surfactant will be transported across the oil−water interface, since the partition coefficient of a surfactant

(22) Gilchrist, A.; Dystr, K. N.; Moore, I. P. T.; Nienow, A. W.; Carpenter, K. J. *Chem. Eng. Sci.* **1989**, *44*, 2381.

(23) Sherman, P. *J. Soc. Chem. Ind. (London)* **1950**, *69*, Suppl. No. 2, S70.

(24) Brooks, B. W.; Richmond, H. N. *Colloids Surf.* **1991**, *58*, 131.

(25) Brooks, B. W.; Richmond, H. N. *Chem. Eng. Sci.* **1994**, *49*, 1065.

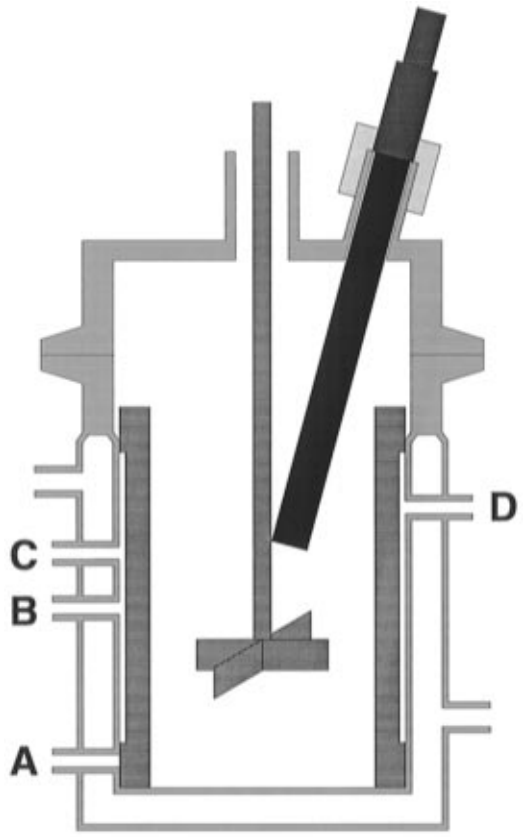

Figure 6. Mixing vessel used in our experiments. A, dispersed phase inlet; B, bypass inlet; C, bypass outlet; D, emulsion outlet.

Table 1. Dimensions of the Mixing Vessel (in mm)

vessel height	173
vessel diameter	110
height above vessel bottom	
A: dispersed phase inlet	9
B: bypass inlet	59
C: bypass outlet	77
D: emulsion outlet	92
stirrer position (above vessel bottom)	47
stirrer blade height	10
stirrer blade width	22
stirrer blade tilt angle (deg)	15
conductivity probe position (above vessel bottom)	109
conductivity probe diameter	12
conductivity probe tilt angle (deg)	22
baffle height	126
baffle width	10
baffle gap	2

is seldom equal to unity. Mass transfer across the interface in emulsions is known to induce positive or negative gradients in the interfacial tension along draining films, depending on the direction of transport.[26] A positive gradient in interfacial tension tends to enhance coalescence and destabilize an emulsion; a negative gradient can slow down the coalescence process and stabilize an emulsion. Neither in our experiments nor in those of other researchers[24,25] have significant stabilizing or destabilizing effects due to surfactant transfer been observed. The partition equilibrium is disturbed by the incoming droplets. As far as our experiments are concerned, the residence time of these droplets in the vessel is very large ($\sim 10^4$ s). It is therefore expected that the partition equilibrium is maintained under a (very slowly) changing volume fraction.

Results and Discussion[27]

The results of a typical phase inversion experiment are shown in Figure 7. Adding water to oil, the conductivity

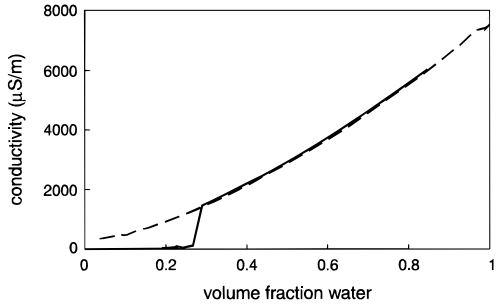

Figure 7. Conductivity as a function of the volume fraction of water in phase inversion experiments, at 1500 rpm stirrer speed and 0.66 mL/s dispersed phase addition rate. Solid line, water added to *n*-hexane; broken line, *n*-hexane added to water.

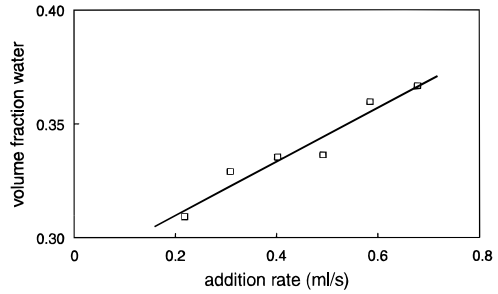

Figure 8. Phase inversion point as a function of water addition rate from W/O to O/W phase inversion experiments, at 1500 rpm stirrer speed.

of the emulsion remains nearly zero until a volume fraction of 37% water is reached. At 37%, the conductivity jumps to a higher value and increases further gradually with increasing volume fraction water. Clearly, an initial water in oil (W/O) emulsion inverts at 37% water to an oil in water (O/W) emulsion. Adding oil to water, the conductivity gradually decreases but never jumps. The O/W emulsion remains intact beyond 63% oil, and inversion could not be observed even up to 97% dispersed phase. Higher volume fractions could not be reached, because it takes infinite time in a CSTR to reach a volume fraction of 100%.

The values for the conductivity as a function of the volume fraction of dispersed phase are in agreement with the theoretical predictions from Bruggeman:[28]

$$\frac{K - K_d}{K_c - K_d}\left(\frac{K_c}{K}\right)^{1/3} = 1 - \phi_d \qquad (22)$$

Clearly, the inversion from W/O to O/W is an example of easy inversion. Figure 7 also shows a hysteresis gap, between 37% water and <3% water. The experimental results are in qualitative agreement with our calculations, as presented in Figures 1 and 2: inversion at relatively low fractions (37% experimentally, 26% calculated) for easy inversion, and no inversion (up to very high volume fractions) for difficult inversion.

Figure 8 shows the influence of the water addition rate on the phase inversion point for inversion from W/O to O/W, at a stirrer speed of 1500 rpm. The inversion point increases slightly with increasing addition rate. Again, this is in qualitative agreement with the calculation results presented in Figure 4. When the results are compared quantitatively, addition rates varying from 0.22 to 0.68 mL/s correspond to $d\phi/dt = 0.00013-0.00041$ s^{-1} at $t = 0$,

(26) Hartland, S.; Jeelani, S. A. K. *Colloids Surf. A* **1994**, *88*, 289.

(27) The experiments have been discussed briefly in: Stein, H. N. *The Preparation of Dispersions in Liquids*; Marcel Dekker, Inc.: New York, 1995.

(28) Bruggeman, D. A. G. *Ann. Phys.* **1935**, *24*, 636.

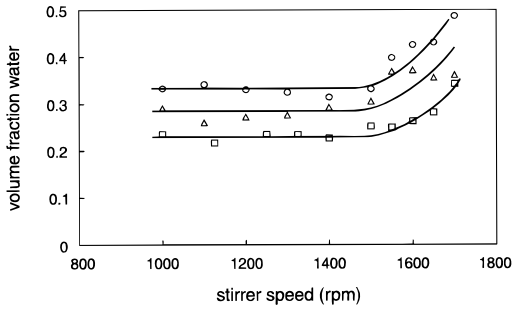

Figure 9. Phase inversion point as a function of stirrer speed from W/O to O/W phase inversion experiments, at water addition rates of 0.13 (squares), 0.40 (triangles), and 0.66 mL/s (circles).

decreasing linearly with ϕ as the experiment proceeds. There is no quantitative agreement, neither in the absolute value of the inversion point (~34% experimentally, ~27% calculated) nor in the inversion point shift upon doubling the addition rate (~3% experimentally, ~1% calculated).

Figure 9 shows the influence of the stirrer speed on the inversion point, at three water addition rates. Until approximately 1500 rpm, the inversion point is nearly independent of the stirrer speed, which is in qualitative agreement with the calculations presented in Figure 1. At higher stirrer speeds, the inversion point increases with increasing stirrer speed, an effect that is not predicted by our calculations. This effect may be attributed to an overestimate of the coalescence probability. For easy inversion, the coalescence probability was assumed to be equal to one in all cases. As can be seen from eq 10, the interaction time t_i decreases with increasing energy dissipation and, therefore, with increasing stirrer speed. This may result in a lower coalescence probability, as soon as the interaction time becomes on the order of the drainage time (which is in general relatively small in the case of easy inversion). In reality, the coalescence rate may be lower than predicted for high stirrer speeds, and the inversion point will actually be higher. Indeed, our calculations show that if a coalescence efficiency of 80% were assumed instead of 100%, the inversion point would increase from 26% to 30%.

A final point that deserves our attention here is the role of multiple emulsions in phase inversion. Close to the inversion point in easy inversion, say from A/B to B/A, the conditions for the formation of an B/A/B emulsion are very favorable: primary droplets of A in B are quite large, and the secondary B droplets dispersed in the primary A droplets are in their preferred morphology (locally a B/A emulsion). Experiments by Brooks and Richmond[24] have shown that the existence of multiple emulsions greatly aids phase inversion. Emulsions, close to the inversion point, were subjected to agitation−settling cycles. Upon settling, primary A droplets coalesce rapidly. The phases that separate appear to be a B/A emulsion and an excess B phase. Reagitation of the mixture will again redisperse droplets of B/A in B. After a number of cycles, agitation will produce a B/A emulsion. Reproducing these experiments, we have found exactly the same behavior for our system, water/*n*-hexane/nonylphenol hexaethoxylate.

In a later paper,[25] Brooks and Richmond presented a mechanism for catastrophic phase inversion in which multiple emulsions play a key role. It is based on an early concept by Ostwald,[29,30] who stated that phase inversion will occur as soon as close packing of the (spherical) droplets is reached. For a monodisperse emulsion, this would be at a volume fraction of 74%; in polydisperse systems, the critical volume fraction is even higher. Catastrophic inversion can occur at lower volume fractions, as a result of a substantial fraction of the continuous phase being trapped in the dispersed phase forming a multiple emulsion. The effective volume fraction of the dispersed phase is much higher than the actual volume fraction of the dispersed phase component, and a state of close packing can be reached. The capture of continuous phase droplets into the dispersed phase may be the reason for the delay in phase inversion observed by Gilchrist et al.[22]

Although we do believe that the formation of multiple emulsions substantially facilitates catastrophic phase inversion, it is very unlikely that it is required that a state of close packing is reached for the emulsion to invert. The model presented in this paper has shown that, without taking into account an increase in effective volume fraction of the dispersed phase, the droplet size will diverge above a volume fraction of 26.4%. This means that all droplets will coalesce long before a state of close packing is reached. The model also predicts a delay in phase inversion, because of the time needed for the droplets to grow. Therefore, we support another mechanism for catastrophic phase inversion, namely, that inversion takes place as soon as the emulsion breaks down as a result of divergence of the stationary droplet size. In most cases, breakdown of the emulsion will not lead to phase separation, but instead the reverse emulsion will be formed by simultaneous direct emulsification.

Conclusions

A simple model for the evolution of the number mean droplet size, based on coalescence and breakup kinetics, can account for many experimental features observed in catastrophic phase inversion. Hysteresis is predicted on the basis of two different inversion mechanisms that are involved, depending on the direction of the process. The model further predicts the inversion point to be independent of the stirrer speed, which is confirmed experimentally in the low-rpm regime. Also, an increase of the inversion point with increasing stirrer speed was calculated and verified experimentally, although the experiments show a stronger increase than the model predicts. While qualitative agreement is found, the absolute values of the inversion point could not be accurately predicted. Clearly, the simple model lacks some necessary, more advanced features:

1. Instead of grouping three classes of droplet sizes back into one after each time step, we should allow for polydispersity. The population balance, i.e., the set of equations describing transitions between classes of droplet sizes, should be solved.

2. The present model assumes the turbulent energy dissipation to be equally distributed over the vessel. In reality, however, there is a zone of high ϵ around the stirrer, where breakup dominates, and a more quiescent zone where coalescence dominates.

3. As the increase of the inversion point with impeller speed has already indicated, the assumption of a coalescence probability of 100% in the case of easy inversion is not very realistic, especially at higher stirrer speeds. With the coalescence probability in difficult inversion derived from the Reynolds drainage equation (eq 1), a coalescence probability in easy inversion may be derived similarly from eq 4.

List of Symbols

a	radius of the flattened area between two draining droplets, m
A	Hamaker constant, J

(29) Ostwald, W. *Kolloid Z.* **1910**, *6*, 103.
(30) Ostwald, W. *Kolloid Z* **1910**, *7*, 64.

B proportionality constant (ref 13)
$c_{0,c}$ equilibrium concentration of the emulsifier in the continuous phase, mol m^{-3}
C_1 proportionality constant (eq 8)
d droplet diameter, m
D_c bulk diffusion coefficient of the emulsifier in the continuous phase, m^2 s^{-1}
D_s surface diffusion coefficient of the emulsifier, m^2 s^{-1}
D_{imp} impeller diameter, m
F external force, N
h film thickness, m
h_0 film thickness at the start of the drainage process ($t = 0$), m
h_c critical film thickness (at film rupture), m
k Boltzmann constant (1.38×10^{-23} J K^{-1})
K conductivity, S m^{-1}
K_c conductivity of the continuous phase, S m^{-1}
K_d conductivity of the dispersed phase, S m^{-1}
$n(d)$ concentration of droplets of size d, m^{-3}
n_0 electrolyte concentration, m^{-3}
N_{imp} impeller speed (revolutions per second), s^{-1}
P coalescence probability
ΔP external pressure, Pa
$R_b(d)$ breakup rate of droplets of size d, m^{-3} s^{-1}
$R_c(d)$ coalescence rate of droplets of size d, m^{-3} s^{-1}
t time, s
t_d drainage time, s
t_i interaction time, s
T temperature, K
v approach velocity, m s^{-1}
V drainage velocity, m s^{-1}
V_0 Reynolds drainage velocity, m s^{-1}
z ion valence

Greek Symbols

Γ_0 equilibrium surface concentration of the emulsifier, mol m^{-2}
ϵ turbulent energy dissipation rate, m^2 s^{-3}
ϵ^e correction factor for internal flow in the droplets during drainage
ϵ^f correction factor for emulsifier transport during drainage
ϵ_0 permittivity of vacuum (8.85×10^{-12} C V^{-1} m^{-1})
ϵ_r relative dielectric constant
κ Debye−Hückel parameter, m^{-1}
μ_c viscosity of the continuous phase, Pa s
μ_d viscosity of the dispersed phase, Pa s
Π disjoining pressure, Pa
σ interfacial tension, N m^{-1}
σ_0 equilibrium interfacial tension, N m^{-1}
τ residence time in the vessel, s
ϕ volume fraction
ψ_0 surface potential, V
ψ_m midplane potential, V

LA950379G